Plant Physiology®

Interplay between ARABIDOPSIS Gβ and WRKY transcription factors differentiates environmental stress responses

Kulaporn Boonyaves [ID] ,[1,2,]* Ting-Ying Wu [ID] ,[1] Yating Dong[1] and Daisuke Urano [ID] [1,2,3,]*

1 Temasek Life Sciences Laboratory, Singapore 117604, Singapore
2 Singapore-MIT Alliance for Research and Technology (SMART), Singapore 138602, Singapore
3 Department of Biological Sciences, National University of Singapore, Singapore 117558, Singapore

*Author for correspondence: kulaporn@tll.org.sg (K.B.), daisuke@tll.org.sg (D.U.)
K.B. conceived the whole project, designed and executed experiments, analyzed data, and wrote the manuscript. T.-Y.W. analysed the public transcriptome dataset and motif enrichment. Y.D. identified differentially expressed genes and performed DEGs clustering. D.U. conceived and supervised the project and edited the manuscript.
The author responsible for distribution of materials integral to the findings presented in this article in accordance with the policy described in the Instructions for Authors (https://academic.oup.com/plphys/pages/General-Instructions) is: Daisuke Urano (daisuke@tll.org.sg).

Abstract

Different environmental stresses often evoke similar physiological disorders such as growth retardation; however, specific consequences reported among individual stresses indicate potential mechanisms to distinguish different stress types in plants. Here, we examined mechanisms to differentiate between stress types in Arabidopsis (*Arabidopsis thaliana*). Gene expression patterns recapitulating several abiotic stress responses suggested abscisic acid (ABA) as a mediator of the common stress response, while stress type-specific responses were related to metabolic adaptations. Transcriptome and metabolome analyses identified Arabidopsis Gβ (AGB1) mediating the common stress-responsive genes and primary metabolisms under nitrogen excess. AGB1 regulated the expressions of multiple WRKY transcription factors. Gene Ontology and mutant analyses revealed different roles among WRKYs: WRKY40 is involved in ABA and common stress responses, while WRKY75 regulates metabolic processes. The AGB1–WRKY signaling module controlled developmental plasticity in roots under nitrogen excess. Signal transmission from AGB1 to a selective set of WRKYs would be essential to evoke unique responses to different types of stresses.

Introduction

Various signaling pathways and transcriptional regulators alter their activities when plant cells are exposed to stress. Some are versatile stress regulators that are commonly activated by many different stresses, while others are engaged in specific types of stresses. The general or specific stress responses lead to adjustments in metabolism, growth, and development that could exhibit similar or diverse phenotypic alterations among different stress types. Regulation of transcription factors (TFs) is known to control those adjustments, but an upstream mechanism to discriminate stress types remains elusive. This study demonstrates the function of G protein signaling networks in differentiating stresses and its association with a distinct set of WRKY TFs in common or specific stress responses.

Different environmental stresses often induce similar cellular responses, such as a release of amino acids and sugars upon oxidative damage, a decrease in photosynthetic

Open Access

efficiency, and changes in the primary metabolites accumulation (Cui et al., 2019; Heinemann and Hildebrandt, 2021; Savchenko and Tikhonov, 2021). These common responses to stress guide growth retardation and cellular protection mechanisms that are central to developmental plasticity under stress conditions (Cramer et al., 2011; Akram et al., 2019). In addition to these common responses, plants produce unique and distinct cellular responses specific to individual stress types. The specific responses generally involve metabolic adjustments like osmolyte accumulation against a high ionic level in soil, and intake/exclusion control mechanisms like transporters for nutrients and toxic minerals (Hu and Schmidhalter, 2005; Yastreb et al., 2016). Induction of the common response in combination with specific responses is essential to ensure the survival and fitness of plants under stress. The common response has been postulated to be controlled with hormones and other chemical cues. Auxin and gibberellic acid determine tissue elongation rate upon environmental fluctuations, while ABA, ethylene, and salicylic acid regulate a plethora of stress and senescence-related genes (Verma et al., 2016; Zhang et al., 2019). Integration of stress-related transcript profiles in Arabidopsis (*Arabidopsis thaliana*) revealed number of universal stress response genes including genes related to ABA and jasmonic acid (Ma and Bohnert, 2007). Arabidopsis genetics studies have shown a selective activation of TFs that underlies specific responses. For example, DEHYDRATION RESPONSIVE ELEMENT-BINDING PROTEIN/C-REPEAT BINDING FACTOR(DREB/CBF) 1 or DREB2 is expressed selectively under low temperature or drought respectively, although regulates similar stress-associated genes (Shinozaki and Yamaguchi-Shinozaki, 2000). Similarly, we and other groups demonstrated a selective induction of WRKY TFs upon high salinity, pathogen infection, and other stresses (Xu et al., 2006; Tao et al., 2011; Wu et al., 2021).

An upstream signaling mechanism that integrates and guides the common and stress-specific TF activations remains unclear. Heterotrimeric G protein, composed of Gα, Gβ, and Gγ subunits, serves as a central regulator for various environmental responses (Offermanns, 2003). Among the three subunits, Gβ is encoded as a single copy gene in Arabidopsis, thus the knockout of *Arabidopsis Gβ* (*AGB1*) is considered to be the genetic ablation of heterotrimeric G protein complex (Urano et al., 2013). Arabidopsis *agb1* null alleles increase sensitivity to high salinity, drought, low temperature, macro, and micronutrient deficiency, and pathogen infection (Urano et al., 2013; Yu and Assmann, 2015; Wu et al., 2020), hence showing a compact rosette under stresses. However, root growth was reduced to a similar extent in wild-type and *agb1* alleles under abiotic stresses (Yu and Assmann, 2015; Liang et al., 2018). The different growth reduction levels between shoots and roots would be linked to tissue-specific regulations of primary metabolite fluxes downstream of AGB1 (Mudgil et al., 2016; Urano et al., 2016b). The *agb1* allele is also hypersensitive to ABA during seed germination, suggesting that ABA may similarly be a mediator of general stress sensing by AGB1 (Pandey et al., 2006). On the other hand, gene expression analysis revealed that the *agb1* allele controls the expression of genes specific to each of individual stresses (Pandey et al., 2010; Wu and Urano, 2018). A genetic complementation assay revealed that AGB1 mediates stress-specific gene expression through WRKY25 or WRKY33 under zinc and iron stresses (Wu et al., 2020) and through WRKY54 under pathogen infection (Kalde et al., 2007). Taken together, these previous studies have implied possible mechanisms wiring the stress response phenotypes in the *agb1* allele, transcriptional regulations, and primary metabolism alterations.

In this study, we present in Arabidopsis roots that AGB1 controls primary metabolisms downstream of a selective set of WRKY TFs. This metabolic adjustment is associated with the developmental plasticity of roots under excessive nitrogen availability. Our research began with transcriptome meta-analysis and identification of ABA signaling-related genes highly enriched in the analyzed abiotic stress transcriptomes. Gene ontology (GO) analysis indicated that each of the stress transcriptomes is associated with distinct metabolic processes depending on stress types. Our in-house transcriptome and metabolome results identified that AGB1, WRKY40, and WRKY75 control primary metabolism and developmental plasticity in Arabidopsis roots under excessive nitrogen availability. Nitrogen excess induced both ABA- and metabolite-related genes in wild-type, but these transcriptional changes were misregulated in *agb1-2*, *wrky40*, and *wrky75* alleles. *WRKY40* was more related to ABA signaling-related genes and *WRKY75* controlled genes more specific to nitrogen responses. The *35S::WRKY75* rescue line in the *agb1-2* background showed a partial rescue in the expression of metabolic and ABA-related genes set. We propose that signal transmission from Gβ to WRKY TFs is an important mechanism to integrate and coordinate both the general and specific responses that define primary metabolic activities and developmental strategy in roots under stress conditions.

Results

General and specific responses to multiple abiotic stresses in Arabidopsis roots

We combined and analyzed 23 publicly available transcriptomes studying a variety of abiotic stresses in Arabidopsis roots. The meta-analysis yielded 3,598 differentially expressed genes (DEGs, P-value $<$ 0.05 as cutoff) controlled by at least one of cold, drought, hypoxia, heat, osmotic, and salt stresses (Figure 1A). GO analysis of biological process demonstrated that DEGs specific to salt, high osmolarity, or heat contained a greater number of significant GO terms than those specific to other abiotic stresses (Supplemental Figure S1 and Supplemental Table S1). Highly significant GO terms unique to the three stresses were related to primary metabolisms, for instance, nitrogen compound- and cellular macromolecule-metabolic processes (Supplemental Figure S1). We next focused on DEGs controlled by at least two
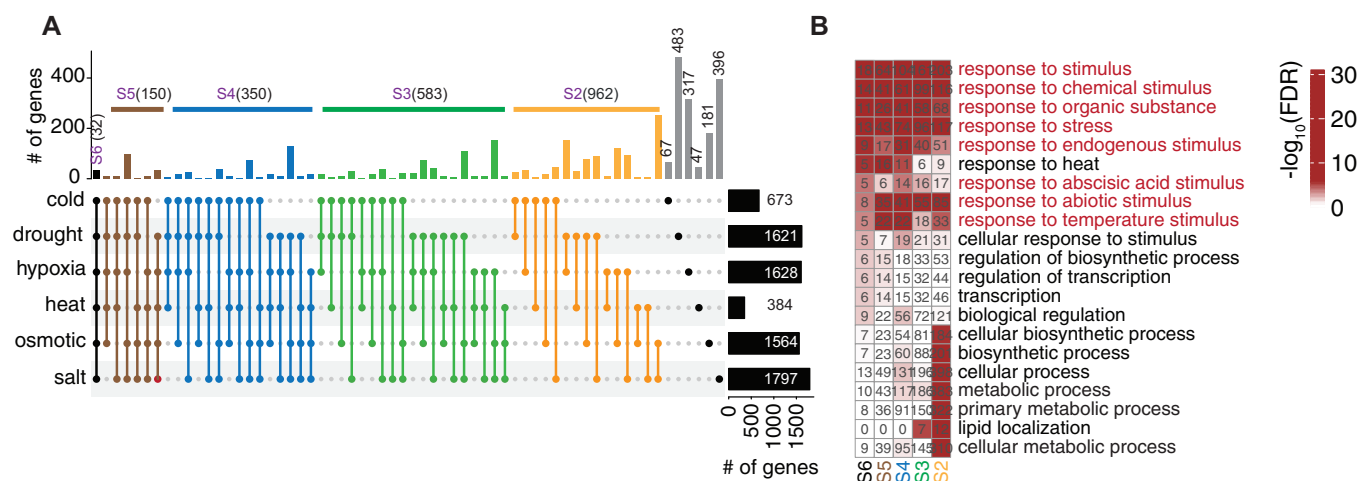
Figure 1 DEGs in response to distinct or multiple types of abiotic stresses. A, Upset plots showing the number of DEGs in response to cold, drought, hypoxia, heat, osmotic, and salt stress. Each column corresponds to a possible intersection between the abiotic stress datasets. The colored dots and lines indicate the sets that are part of the intersection. Bar graphs on the right panel represent the total number of DEGs identified in each stress type. Bar graphs on the upper panel represent the size of each intersection, which corresponds to the number of DEGs that commonly responded to more than one stress type (S2–S6), and the size of individual abiotic stress. These are color-coded according to the number of intersections between datasets (S6: black, S5: brown, S4: blue, S3: green, S2: yellow, S1: gray). Numbers in black represent numbers of identified DEGs. B. GO terms (Biological process, BP) enriched in commonly responsive DEGs (S2–S6, from the upper bar graph in A). The color scale represents $-\log_{10}$(FDR). The numbers in each cell represent the numbers of DEGs associated with GO terms shown on the right. GO names in red indicate GO terms that are significantly enriched (FDR < 0.05) in all stresses analyzed.

independent stress treatments (Supplemental Figures S2, S3, S4, S5, and S6; Figure 1B). The multi-stress DEGs contained significant GO terms for responses to stimulus, chemical stimulus, organic substances, stress, endogenous stimulus, ABA stimulus, abiotic stimulus, and temperature stimulus. These were further compared with responses caused by excessive nitrogen availability (high nitrogen [HN]), which causes disrupted primary metabolism, oxidative stress, and root growth retardation (Wei et al., 2009; Zou et al., 2012; Kong et al., 2017; Lan et al., 2020). We generated transcriptomic data of root samples in response to HN and our inhouse data indicated that a total of 2,925 genes were differentially expressed by HN in wild-type roots (Supplemental Figure S2A). Among them, 1,747 DEGs were overlapped with the DEGs found in the meta-analysis, while 1,178 genes were specifically up- or downregulated by HN. The HN-specific DEGs contained significant GO terms related to metabolic pathways, particularly in nitrogen and carbon metabolism (Supplemental Figure S2B), whereas the HN-common DEGs had significant GO terms for stress, hormone, and ABA responses (Supplemental Figure S2C). Taken together, these transcriptional analyses revealed two distinct groups of DEGs under stress responses: one related to universal stress response and the other unique to individual stress types like nitrogen and carbon metabolisms under excessive nitrogen.

The *agb1* allele regulating common and HN-specific stress responses

The involvement of G protein in the two distinct stress responses was examined by comparing root transcriptomes between Col-0 and *agb1-2* with or without HN. Based on the linear model of genotype × environment, 676 and 1,706 genes were identified as genotypic deviation DEGs and gene-by-environment interaction (G × E) genes, respectively (Figure 2A). Roughly one-fourth of the *agb1-2*-regulated genes overlapped with abiotic stress-related DEGs obtained from the earlier meta-analysis (Figure 2A). To visualize the individual and mixed effects of genotypic and environmental deviations, the 1,706 G × E DEGs were further classified into 10 groups (G) based on expression patterns (Figure 2B; Supplemental Table S2). Those G × E DEGs were largely unique to HN rather than overlapping with abiotic stress-related genes (48%–89%, Figure 2A). Interestingly, more than 50% of the G × E DEGs in all groups except G4 and G8 exhibited differential expression between Col-0 and *agb1-2* at the control condition (Figure 2B). Instead, G8 showed genotypic differences only at the HN condition (Supplemental Table S3). The clustering analysis revealed two patterns: (1) either up-regulated in *agb1-2* or down-regulated in Col-0 by HN in G1, G2, G4, G7, and G9 and (2) either up-regulated in Col-0 or down-regulated in *agb1-2* by HN in G3, G5, G6, G8, G10. The HN-specific genes contained significant GO terms for the metabolic process (G1, G2, and G7) and several primary metabolisms including amino acids and aromatic compounds (G4, Figure 2C). In contrast, common stress response genes in G8 had significant GO terms for response to ABA and stress, suggesting the involvement of *AGB1* in both ABA and metabolic responses (Supplemental Figure S3). We next focused on metabolic genes extracted from AraCyc database (Schläpfer et al., 2017) and analyzed the activation/inactivation of individual metabolic pathways.
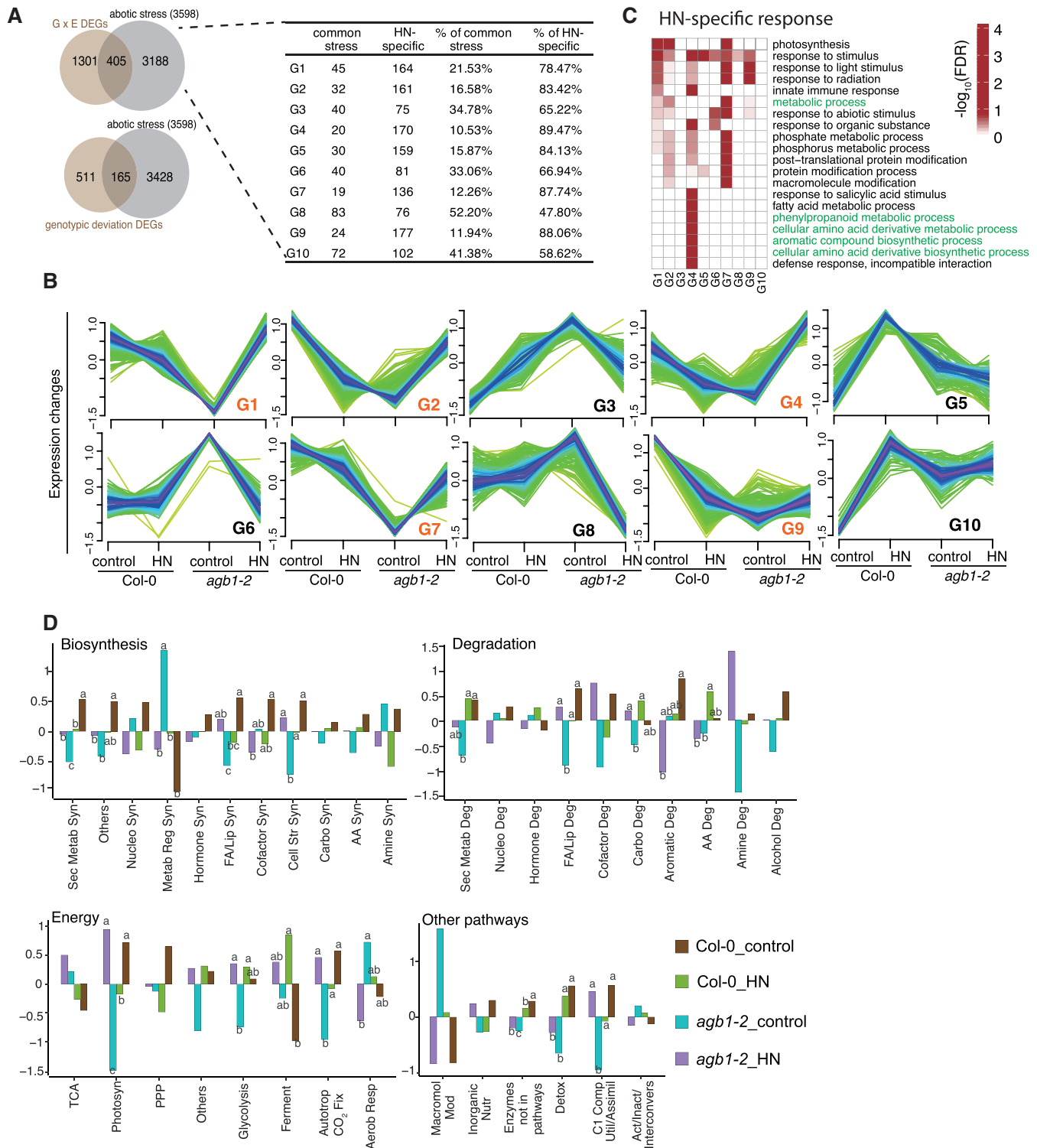
Figure 2 Regulation of AGB1 in primary metabolisms upon HN treatment. A, Venn diagram and table representing the overlap of DEGs responding to HN with other abiotic stresses. G × E and genotypic deviation DEGs were obtained based on the linear model of G × E. Abiotic stress DEGs refer to the genes identified from meta-analysis in Figure 1A. G1–G10 in the table are groups of G × E DEGs as clustered using fuzzy c-means. B, Gene expression patterns of DEGs in G1–G10. Expression changes in y-axis represent Z-score of $\log_2$-normalized read counts of DEGs. Line graphs represent expression patterns of each individual gene. Line colors represent membership values that range from 0 to 1, indicating the score of gene belonging to each cluster core (G1–G10). DEGs with membership value ⩾ 0.9, 0.7, and 0.5 are designated as pink, dark blue, and light blue, respectively. Green lines represent DEGs with membership value < 0.5. G1, G2, G4, G7, and G9 in orange represent either up-regulated in *agb1-2* or down-regulated in Col-0 by HN. G3, G5, G6, G8, and G10 in black represent either up-regulated in Col-0 or down-regulated in *agb1-2* by HN. C, GO enrichment analysis of DEGs belonging to HN-specific response of each gene group. The color scale represents $-\log_{10}$(FDR). GO names in green indicate GO terms related to primary metabolism, particularly in amino acids. D, Expression of metabolism-related genes. DEGs involved in

(continued)

The *agb1-2* allele largely changed primary metabolisms including biosynthesis and degradation of fatty acid, biosynthesis of metabolic regulators, photosynthesis, carbon fixation, and C1 compound utilization at the control condition (Figure 2D). HN treatment enhanced gene expression related to degradation of amino acid in Col-0, whereas photosynthesis and C1 compound utilization in *agb1-2*. These results suggest that primary metabolisms in *agb1-2* were misregulated at the control condition, which generally mimics metabolic adjustments observed under nitrogen excess.

Root growth plasticity under excessive nitrogen availability in the *agb1* allele

Plant roots show high phenotypic plasticity in response to insufficient or excessive nutrient resources (López-Ruiz et al., 2020). Here, we observed root developmental phenotypes under four different nitrogen conditions (Figure 3A). Primary root growth was inhibited by an HN supply (Figure 3B); however, the *agb1-2* mutation mitigated the inhibitory effect (Figure 3C). Expression of *AGB1* under its native promoter in the *agb1-2* mutant (*AGB1/agb1-2*) canceled the mitigation, and the plant roots were sensitive to HN stress (Supplemental Figure S4, A and B). Nitrogen concentrations did not affect lateral root density in both Col-0 and *agb1-2* (Supplemental Figure S5). We also estimated root growth in other G protein mutants; *gpa1-2*; *agg3-3*; *agg1-1|agg2-1*; *agg triplet*; *xlg1,2,3*; and *gpa1-3|xlg1,2,3*. The *agg1-1|agg2-1*; *agg triplet*; and *gpa1-3|xlg1,2,3* exhibited longer primary roots than Col-0 under excessive nitrogen condition (Supplemental Figure S6), similar to that of the *agb1-2* allele. Nitrogen excess reduced leaf area but not chlorophyll and nitrate contents in Col-0 seedlings (Supplemental Figure S7, A and B). The *gpa1-3*; *xlg1,2,3*; and *gpa1-3|xlg1,2,3* exhibited significantly smaller leaf area than Col-0 under control conditions (Supplemental Figure S7B). The *gpa1-3|xlg1,2,3* accumulated higher nitrate content than Col-0 at the control condition (Supplemental Figure S7B). The adverse effect of excessive nitrogen can be lessened by high carbon content in the growth medium, as plants promote metabolic activities toward growth when sufficient carbon is available. This was confirmed in Col-0 by supplementing 0.5% sucrose to HN medium (40-mM NO_3^- + 30-mM NH_4^+), but sucrose did not affect the decline in root elongation in *agb1-2* (Figure 3, D and E). Together with primary metabolite pathway analyses (Figure 2D), we propose that AGB1 modulates root growth rate in response to a nitrogen–carbon balance by controlling the activity of primary metabolism.

Selective regulation of WRKY TFs by AGB1 under HN and stress conditions

Selective activation of TFs is the key to determining specific stress responses, thus we next aimed to identify TF families associated with genotypic (Col-0 vs *agb1-2*) and environmental (control vs HN) interactions. The TF-family analysis revealed only a few TF families (e.g. MYB, MYB-related, and WRKY) over-presented in multiple G × E Groups (Figure 4A; Supplemental Figure S8A). The involvement of these TF families was further supported by putative cis-regulatory elements (pCREs) accumulated in the G × E Group genes (Figure 4B; Supplemental Figure S8B). bHLH, NAC and MYB-related, and NLP TF families are known to be induced with different nitrogen availabilities (Konishi and Yanagisawa, 2013; Xin et al., 2019). Consistent with previous studies, pCREs for bHLH, MYB-related, NAC, and NLP were substantially enriched in the promoter regions of all the 10 Group genes (Supplemental Figure S8B). Interestingly, WRKY-binding motifs were substantially enriched in G1, G2, G4, G7, and G9 where induction of nitrogen-responsive genes was observed only in the *agb1-2* allele but not in Col-0. These results highlight the WRKY family as a potential downstream regulator of *Agb1* under HN and possibly several stresses as well. Indeed, we found that induction of individual WRKYs was highly specific to stress types (Figure 4C). WRKY TFs can be classified into two groups based on their expression patterns (Figure 4C; Supplemental Figure S8C). The first group, containing WRKY18, 22, 33, 38, 40, and 46 showed increased expression with a variety of abiotic stresses including salt, hypoxia, cold, and drought. The other group consists of roughly 90% of WRKYs among which a sub-branch of WRKY45 and 75 exhibited up-regulation in one dataset of salinity treatments. Among them, WRKY40 and 75 and a few other members showed HN-induced expression at different levels between *agb1-2* and Col-0 (right columns, Figure 4C). To demonstrate the HN-responsive functions of these WRKYs, transcriptomic profiles with and without excessive nitrogen were collected from the *wrky40* and *wrky75* single alleles (Figure 5A). The upset plot of DEGs demonstrated a larger number of both up- and down-regulated genes in Col-0 than those in *wrky40* and *wrky75* alleles (Figure 5B). The *wrky75*-specific DEGs contained significant GO terms for oxidation–reduction and metabolic

Figure 2 (Continued)
cellular metabolisms were categorized by AraCYC. Bar graphs represent the average Z-score of log₂ normalized read counts of genes in each category. Letters above bars indicate statistical differences among each metabolic category by one-way ANOVA with a post-hoc Tukey HSD test with adjusted P-value < 0.05. "Sec metab" is secondary metabolite. "Syn" is biosynthesis. Nucleo is nucleoside and nucleotide. "Metab Reg" is the metabolic regulator. "FA/Lip" is fatty acid and Lipid. "Cofactor Syn" is cofactor, carrier, and vitamin biosynthesis. "Cell Str" is cell structure. "Carbo" is carbohydrate. "Aromatic" is aromatic compound. "AA" is amino acid. "Amine" is amine and polyamine. "Alcohol" is alcohol. "Cofactor Deg" is cofactor, prosthetic group, electron carrier degradation. "TCA" is tricarboxylic acid. "Photosyn" is photosynthesis light reactions. "PPP" is the pentose phosphate pathway. "Ferment" is fermentation. "Autotrop CO₂ Fix" is Autotrophic CO₂ Fixation. "Aerob Resp" is aerobic respiration. "Macromol Mod" is macromolecule modification. "Inorganic Nutr" is inorganic nutrient metabolism. "Detox" is detoxification. "C1 Comp Util/Assimil" is C1 compound utilization and assimilation. "Act/Inact/Interconvers" is activation/inactivation/interconversion.
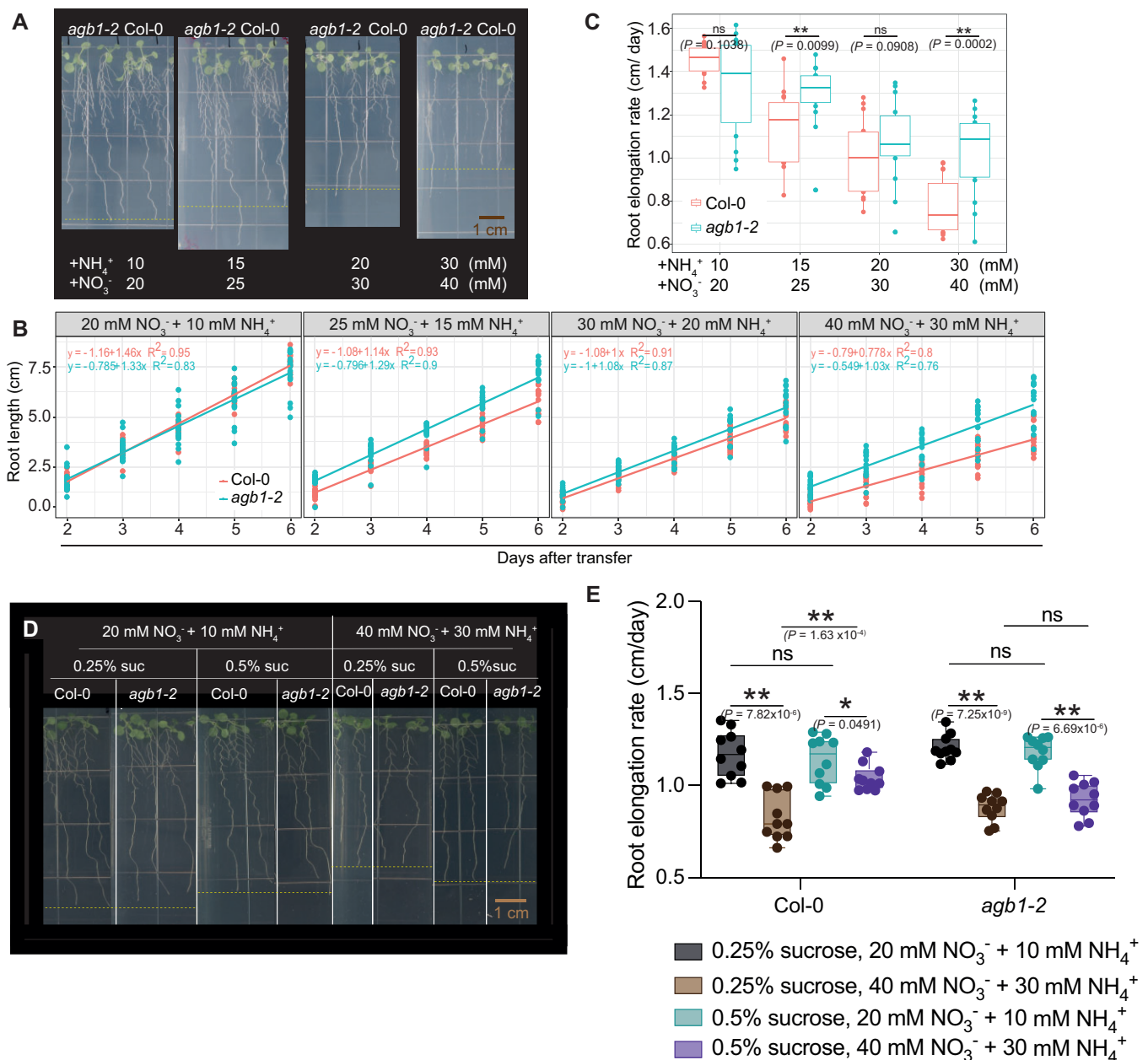
Figure 3 Root growth of *agb1-2* in response to nitrogen and carbon supplies. A, Root phenotype of Col-0 and *agb1-2* in different nitrogen supplies. Dashed lines indicate the position of the longest root of Col-0 in the photo. B, Primary root growth in response to different nitrogen supplies. C, Root elongation rate in four different nitrogen supplies ($n = 16$, two independent experiments). Box limits represent the upper and lower quartiles. Whiskers represent minimum to the lower quartiles and maximum to the upper quartiles. Data points that are outside of 1.5 times interquartile are represented as points and considered as potential outliers and maximum of data. Asterisks (**) represent $P < 0.01$ across genotypes in the same nitrogen supplies. *P*-value is determined by a two-tailed Student's *t* test. D, Root phenotype in different sucrose (suc) supplies under different nitrogen supplied. Dashed lines indicate the position of the longest root of Col-0 in the photo. E, Root elongation rate in different sucrose and nitrogen condition ($n = 10$, two independent experiments). Raw data are represented as points. Box limits represent the upper and lower quartiles. Whiskers represent the minimum to the lower quartiles and the upper quartiles to the maximum. Asterisks (* or **) represent $P < 0.05$ or $P < 0.01$, respectively, across sucrose or nitrogen supplies in the same genotype. *P*-value is determined by a two-tailed Student's *t* test.

process, whereas *wrky40*-specific DEGs were related to metabolic process and response to stimulus, abiotic stress, ABA, and phytohormones (Figure 5C; Supplemental Figure S9A). Quantification of metabolic content revealed that HN enhanced the accumulation of primary metabolites including fructose and galactinol in Col-0 (Figure 5D). The *agb1-2*,

wrky40, and *wrky75* plants accumulated more fructose and galactinol than Col-0 at the control condition (Figure 5D; Supplemental Figure S9B and Supplemental Table S4). Similar metabolites accumulation was found among *agb1-2* and *wrky* mutants upon HN treatment (Supplemental Figure S9C). In addition, we found that both *wrky40* and
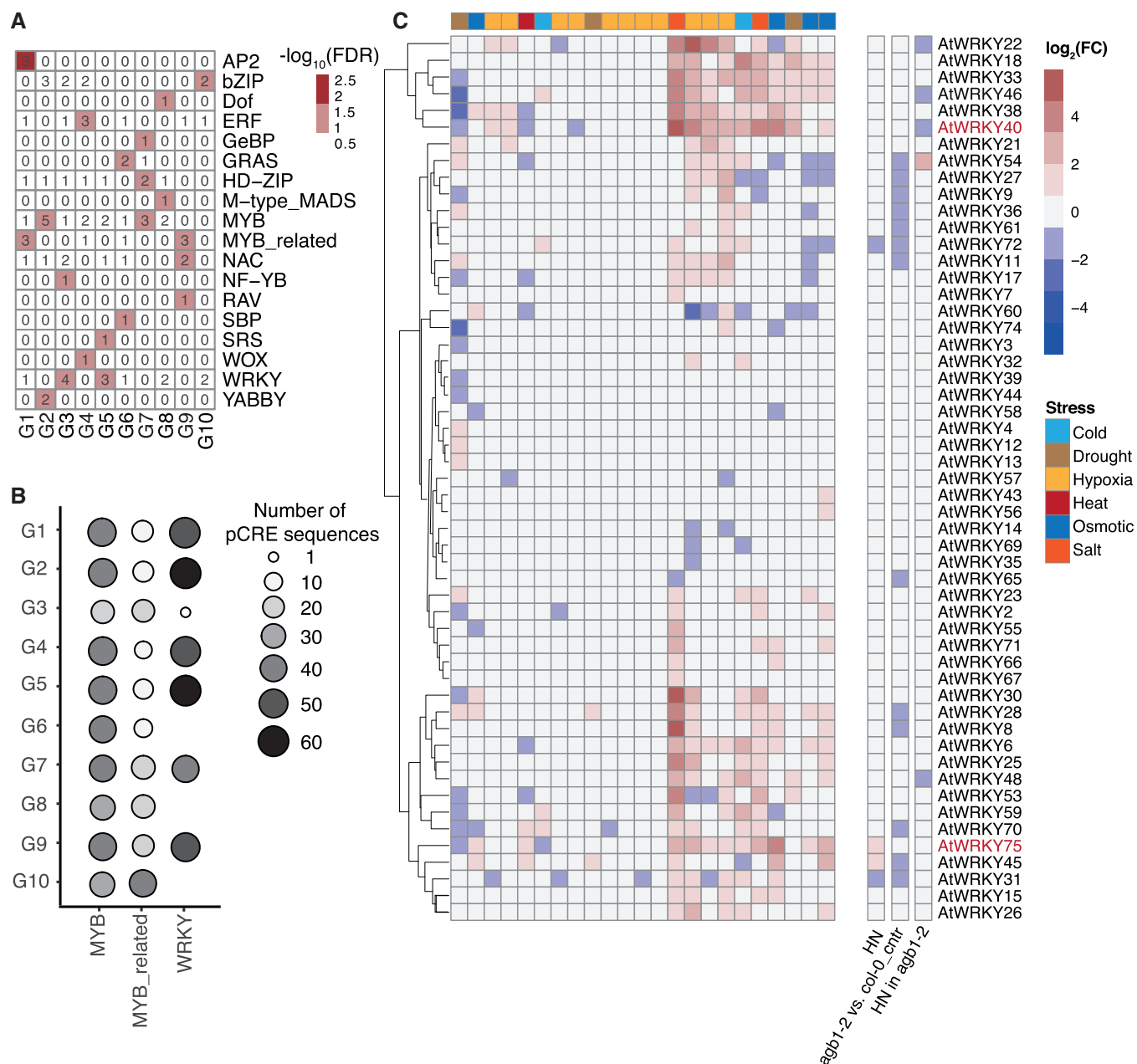
Figure 4 Enrichment of WRKY TFs in response to HN and abiotic stresses. A, Enrichment ($-\log_{10}$(FDR)) of TF families in 10 gene groups (G) derived from Figure 2B. The heatmap presents TF families identified in at least 1 of 10 groups with $-\log_{10}$(FDR) more than 1. B, Bubble plots represent the number of pCREs related to MYB, MYB-related, and WRKY that enriched in the promoter region of genes differentially expressed in 10 gene groups from Figure 2B. Circle size represents the number of pCRE sequences. Enrichment of all TF families and pCRE of all TFs are shown in Supplemental Figure S8, A and B, respectively. C, WRKYs' expression patterns in several abiotic stresses (from Figure 1) and HN stress. Heatmap shows $\log_2$ expression (treatment/control), where red denotes up-regulation and blue indicates down-regulation in each stress condition. Only WRKY TF that showed $|\log_2 FC|$ more than 1 in at least one condition of abiotic stresses are shown. Expressions of all WRKY TFs in abiotic stresses and HN stress are shown in Supplemental Figure S8C.

wrky75 alleles were more tolerant to HN in primary root growth (Figure 5, E and F). These results suggest that both WRKY40 and 75 are involved in HN response by controlling different groups of HN-responsive genes, although both WRKYs are similarly important for metabolic adjustments and root growth control under excessive nitrogen availability.

General and HN-specific stress responses through AGB1 and WRKYs

Our transcriptome and GO analyses suggested two potential mechanisms in how WRKY40 and 75 mediate abiotic stress responses: metabolic adjustments more specific to HN and general stress responses possibly through ABA (Figure 5C). These selective functions of *WRKY40* and *75* were further
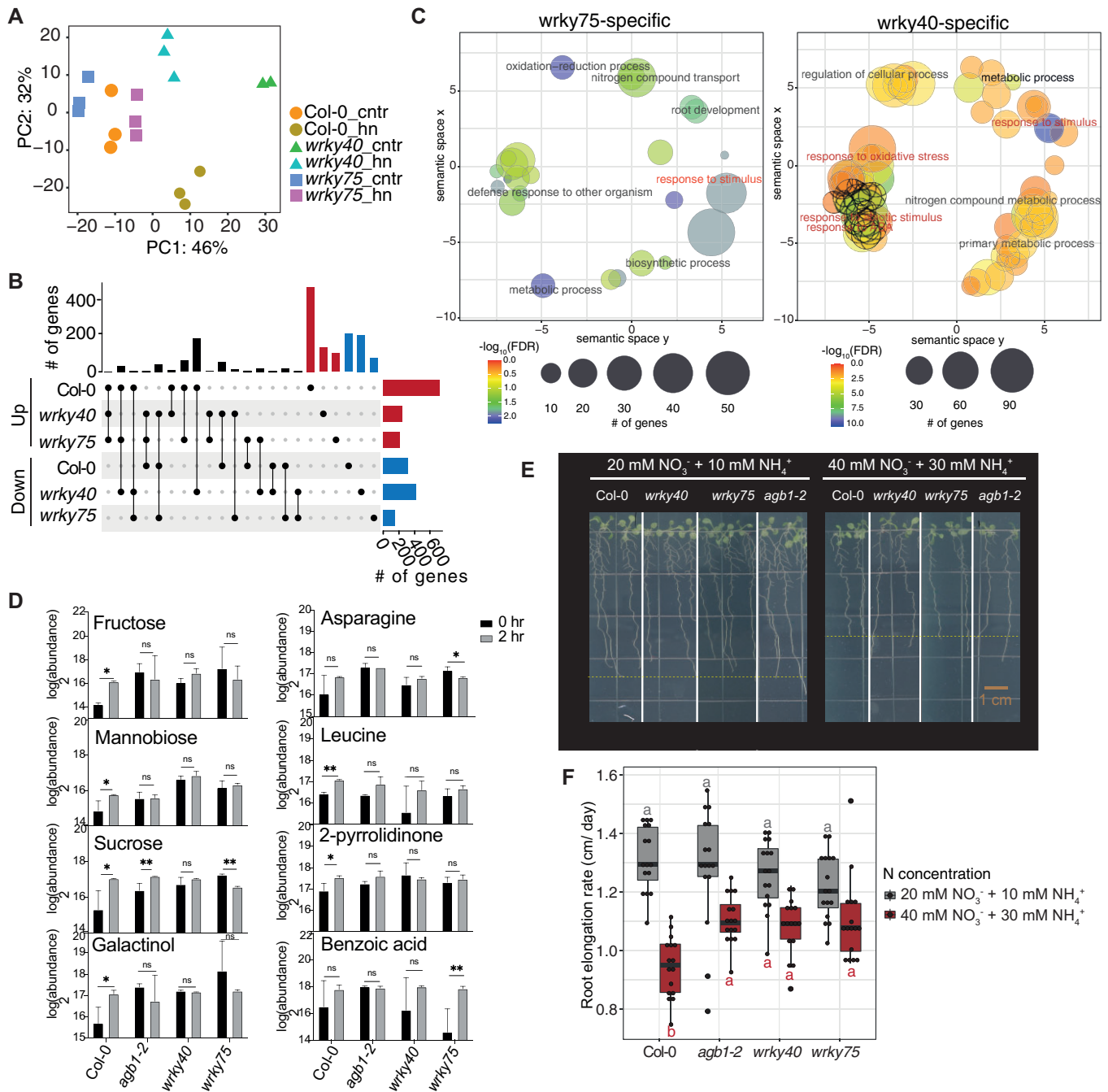
Figure 5 Metabolic response of *wrky40* and *wrky75* to HN. A, Principal component analysis of RNA-seq data of Col-0, *wrky75*, and *wrky40* in response to HN. B, Upset plot represents the number of up-regulated (red) and down-regulated (blue) DEGs in each genotype and overlapped DEGs. C, GO enrichment analysis of *wrky75*-specific and *wrky40*-specific DEGs. Selected GO terms annotated to biological process are shown. The color scale represents −log₁₀(FDR). Dot size represents gene number. GO names in red and black indicate GO terms related to common stress response and metabolisms, respectively. All GO terms annotated to biological process are shown in Supplemental Figure S9A. D, Metabolite content in roots of Col-0, *agb1-2*, *wrky40*, and *wrky75* root at 0 and 2 h after addition of NH_4NO_3 ($n = 3$). Error bars represent standard deviations. Asterisks (* or **) indicate significance at $P < 0.05$ or $P < 0.01$, respectively when compared to 0 h by two-tailed Student's t test. Selected primary metabolites are shown. All metabolite contents and P-value are shown in Supplemental Figure S9B and Supplemental Table S4A. E, Root phenotypes of Col-0, *agb1-2*, *wrky40*, and *wrky75* at different nitrogen supplies. Dash lines indicate the position of the longest root of Col-0 in the photo. F, Root elongation rate in different nitrogen supplies ($n = 16$, two independent experiments). Raw data are represented as points. Box limits represent the upper and lower quartiles. Whiskers represent the minimum to the lower quartiles and the upper quartiles to the maximum. Data points that are outside of 1.5 times interquartile are represented as points and considered as potential outliers and maximum of data. Gray or red letters denote significant differences among genotypes at the control condition or HN supplies, respectively, by one-way ANOVA with a post-hoc Tukey HSD test.

tested with reverse transcription-quantitative PCR (RT-qPCR) of metabolic markers and ABA-related genes under the HN condition or ABA treatment (Figure 6A; Supplemental Figure S10). These markers (e.g. *NITRATE REDUCTASE (NADH)1 (NIA1)*, *GLUCOSE-6-PHOSPHATE DEHYDROGENASE 1 (G6PD1)*, and *ABA-INSENSITIVE 5 (ABI5)* showed similar expression patterns in *wrky75* and *agb1-2* mutants under HN, as supported by hierarchical clustering. Overexpression of *WRKY75* in *agb1-2* (OEWRKY75|*agb1-2*) restored the expression of some metabolic gene markers (e.g. *SUCROSE SYNTHASE 4 (SUS4)*, *NIA1*, *GLUCOSE-6-PHOSPHATE DEHYDROGENASE 3 (G6PD3)*, and *GLUTAMINE-DEPENDENT ASPARAGINE SYNTHASE 1 (ASN1)*), suggesting the presence of AGB1 to WRKY75 pathway controlling metabolic genes under HN. Some of these markers were also induced or repressed by ABA treatment. Highly induced markers under ABA (e.g. *ABI5*, *SUCROSE SYNTHASE 1 (SUS1)*, and *DEHYDRATION-RESPONSIVE ELEMENT-BINDING PROTEIN2A (DREB2A)* showed minimal differences across genotypes, while *agb1-2* exhibited different ABA regulations of some other markers from Col-0. In addition, the RT-qPCR experiment found a combination of genotypes (Col-0 vs *agb1-2*) and extracellular stimuli (HN vs ABA) which defines the selective induction of individual WRKYs (Figure 6B; Supplemental Figure S10). HN induced *WRKY45, 54*, and *75* selectively in Col-0 but not in *agb1-2*; however, ABA treatment oppositely induced the same *WRKY* genes only in *agb1-2* but not in Col-0. ABA also induced *WRKY18* and repressed *WRKY40* only in Col-0. These results suggest an important role of *AGB1* in the selective induction/repression of individual *WRKYs* including *WRKY40* and *75*. Moreover, HN significantly induced ABA accumulation in *agb1-2* and *wrky40* mutants but not in Col-0, *wrky75*, and OEWRKY75|*agb1-2*, suggesting that the overexpression of *WRKY75* could cancel the effect of *agb1-2* mutant (Supplemental Figure S11). Root growth assay showed a reduced sensitivity of *agb1-2* to ABA treatment (Figure 6, C and D). The *wrky40* or *wrky75* roots exhibited ABA sensitivity to a similar extent as Col-0, and OEWRKY75|*agb1-2* did not rescue the low ABA sensitivity phenotype of the *agb1-2* allele. The OEWRKY75|*agb1-2* allele also failed to rescue the HN insensitivity of the *agb1-2* mutant (Figure 6, E and F), implying the existence of additional downstream targets of *AGB1* that define the hormonal and nutritional regulations of root growth plasticity. Taken together, these results suggest AGB1 as a potential definitive factor to enable a selective induction of individual WRKYs upon different types of stresses.

Discussion

Plants utilize both common and specific responses to individual stresses. The meta-transcriptional analysis revealed that abiotic stresses share expressions of ABA signaling and several stress-responsive genes in common, whereas the regulation of metabolic adaptation depends on individual stress types (Figure 1; Supplemental Figure S1). By comparing the

public transcriptome of abiotic stress responses with our in-house HN transcriptome, we found that AGB1 is involved in both common- and specific-stress responses. Loss of AGB1 altered gene expression pattern in response to HN including activation of stress-responsive genes and regulation of primary metabolic process (Figure 2, B and C; Supplemental Figure S3C). Transcriptomic profiling indicated altered metabolic activities in *agb1-2* at control condition (Figure 2D). We also found that loss of AGB1 and other G protein subunits reduced the inhibitory effect of HN on primary root growth (Figure 3; Supplemental Figure S6). We identified WRKY TFs as a downstream regulator of AGB1 signaling and regulating metabolic and ABA response (Figures 4C and 6B). The *agb1-2*, *wrky40*, and *wrky75* mutants showed a relatively higher accumulation of primary metabolites than Col-0 in the control condition and insensitive root growth to HN (Figure 5, D–F; Supplemental Figure S9B). ABA and HN treatment confirmed misregulation of WRKY TFs in *agb1-2* (Figure 6B). Ectopic expression of WRKY75 in the *agb1-2* background partially restored primary metabolic and ABA-related genes in response to HN but not to ABA (Figure 6A). We propose that AGB1 acts as a stress sensor to differentiate stresses by regulating WRKY expression (Figure 6G). Each WRKY regulated metabolic enzymes and stress-responsive genes at different levels.

Selective activation of TFs is essential to enable appropriate stress adaptations. We identified AGB1 and WRKY75 that modulate metabolic adaptations in response to HN (Figures 4 and 6A). The induction pattern of WRKYs under HN and ABA indicates the function of WRKYs in specific-stress responses (Figure 6B). Several genetics studies in Arabidopsis confirmed the stress-specific role of *WRKY* genes, such as WRKY46, 53, and 70 in pathogen response, and WRKY25 and 33 in micronutrient stress and salt stress responses (Hu et al., 2012; Wu et al., 2020, 2021). Our meta-transcriptome analysis also highlighted the expression of common stress-responsive genes shared by several abiotic stresses, possibly mediated by ABA (Figure 1). WRKY40 was reported to function in ABA signaling and bind to promoters of several ABA-responsive genes (Shang et al., 2010). Loss of *AGB1* led to the misregulation of WRKY40 in ABA treatment, suggesting the interplay of AGB1 and WRKY40 in common-stress response. A previous report revealed the function of AGB1 in attenuating proteasome-mediated degradation of BOTRYTIS-INDUCED KINASE 1 (BIK1), a downstream target of WRKY40 (Liang et al., 2016; Birkenbihl et al., 2017). It is noted that the HN treatment did not alter *WRKY40* expression in *agb1-2* as validated by RT-qPCR; therefore, it cannot be concluded whether plants respond to HN via the crosstalk between *AGB1* and *WRKY40*. In addition to ABA response, other phytohormones i.e. ethylene, jasmonic acid, and salicylic acid could modulate WRKY expression upon several stress conditions (Jiang et al., 2017).

Different abiotic stresses often cause similar metabolic adjustments such as sugar accumulation, but transcriptional regulations in these metabolic pathways could differ
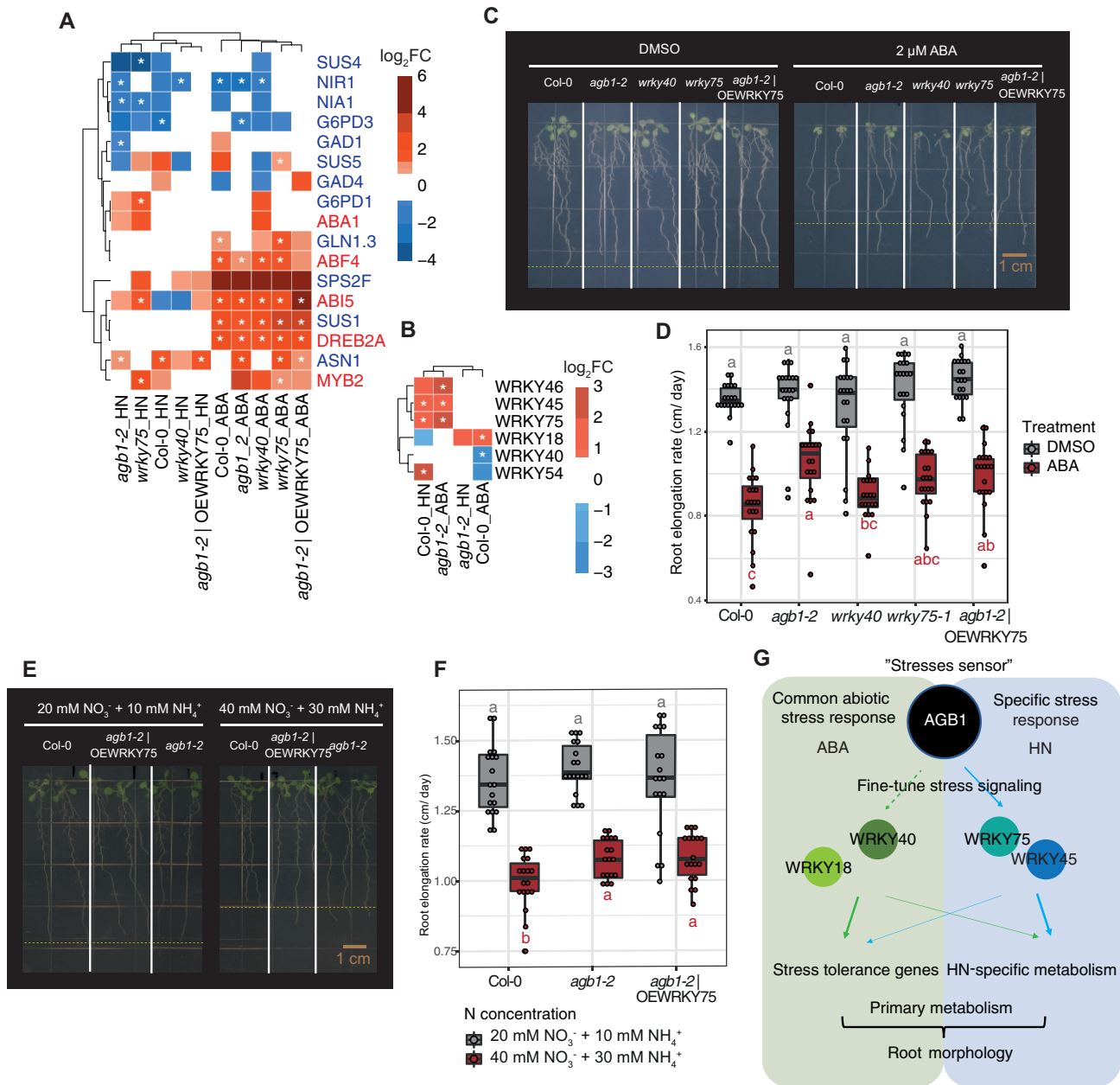
Figure 6 WRKY TFs involved in response to both HN and ABA. A, Quantitative gene expression analysis of metabolic and ABA-related genes in roots of Col-0 and *agb1-2*, *wrky40*, *wrky75*, and OEWRKY75|*agb1-2* in response to HN or ABA treatment (*n* = 3). B, Quantitative gene expression analysis of WRKY TFs in roots of Col-0 and *agb1-2*, in response to HN or ABA treatment (*n* = 3). Asterisks in (A) and (B) indicate the significance of |log$_2$FC| at $P < 0.05$ by two-tailed Student's *t* test. Relative expressions to AtACT2 of all genes are shown in Supplemental Figure S9. C, Root phenotype of Col-0, *agb1-2*, *wrky40*, *wrky75*, and OEWRKY75|*agb1-2* with or without ABA supplement. Dash lines indicate the position of the longest root of Col-0 in the photo. D, Root elongation rate of Col-0, *agb1-2*, *wrky40*, *wrky75*, and OEWRKY75|*agb1-2* in ABA or mock treatment (*n* = 20, two independent experiments). Raw data are represented as points. Box limits represent the upper and lower quartiles. Whiskers represent the minimum to the lower quartiles and the upper quartiles to the maximum. Data points that are outside of 1.5 times interquartile are represented as points and considered as potential outliers and maximum of data. Gray and red letters denote significant differences among genotypes at mock treatment (DMSO) or ABA treatment, respectively, by one-way ANOVA with a post-hoc Tukey's honestly significant difference test. E, Root phenotype of Col-0, *agb1-2*, and OEWRKY75|*agb1-2* at different nitrogen supplies. Dash lines indicate the position of the longest root of Col-0 in the photo. F, Root elongation rate of Col-0, *agb1-2*, and OEWRKY75|*agb1-2* in different nitrogen supplies (*n* = 18, two independent experiments). Raw data are represented as points. Box limits represent the upper and lower quartiles. Whiskers represent the minimum to the lower quartiles and the upper quartiles to the maximum. Data points that are outside of 1.5 times interquartile are represented as points and considered as potential outliers and maximum of data. Gray or red letters denote significant differences among genotypes at the control condition or HN supplies, respectively, by one-way ANOVA with a post-hoc Tukey HSD test. G, A model representing the interplay of AGB1 and WRKY TFs functions upon stress. Green arrows indicate the roles of WKRY TFs in common abiotic-stress responses. Blue arrows indicate crosstalk between AGB1 and WRKY TFs regulating HN responses as suggested by OEWRKY75|*agb1-2*. Dash arrow indicates the possible crosstalk of AGB1 and WRKY TFs in common abiotic-stress response.

depending on stress types. Our meta-transcriptome and GO analyses revealed different metabolic genes regulated by individual stresses (Supplemental Figure S1). For example, HN prompted sugar accumulation (Figure 5E) relevant to transcriptional changes of the photosynthesis pathway (Figure 2D). However, these HN-responsive genes showed only a partial overlap with metabolic genes induced/repressed by other abiotic stresses (Supplemental Figure S2B). The distinct metabolic regulations may be achieved by selective and combinatorial TF inductions. For example, drought and ABA induce rice (Oryza sativa) ONAC095 which regulates sugar accumulation, but cold stress oppositely represses ONAC095 although sugar is highly accumulated at both drought and low temperature (Gounaris, 2001; Huang et al., 2016). In this study, WRKY40 and 75 transcriptionally controlled primary metabolite adjustments at HN (Figure 5C), but the two WRKYs generally function at different stress conditions as exhibited by their distinct stress-induced patterns (Figure 4C). Moreover, a previous study reported the strong induction of WRKY75 upon phosphate deficiency (Devaiah et al., 2007). Because nitrogen and phosphate deficiencies share a common adaptation mechanism to ensure plant nutrient responses (Desnos, 2008; Poza-Carrión and Paz-Ares, 2019), WRKY75 may serve as an important mediator of macronutrients controlling metabolic adjustments (Figure 5C), rather than limited to functions specialized for excessive nitrogen response.

Excessive nitrate application is a significant concern in agriculture. Elevated nitrate concentration ranged from 41.1 to 161. 6 mmol kg^{-1} in certain areas in China (Tang et al., 2014; Gou et al., 2020). Roots display diverse morphologic variations at different levels of ammonium and nitrate excess (Gruber et al., 2013). High residual ammonium level decreases seminal root elongation in rice fields (Hirano et al., 2008; Xuan et al., 2013). Improvement of root system architecture (RSA) for stress tolerance could be critical for developing efficient crops (Koevoets et al., 2016). Transcriptomic and metabolic profiles highlighting primary metabolic activities upon stress could be one of the indicators determining stress resistance in designing better RSA traits. In our study, the agb1-2 and wrky alleles maintained primary root elongation even at the HN condition. The agb1-2 and wrky plants at the control condition partially resembled transcriptional and metabolic status under nitrogen excess such as enhanced biosynthesis of metabolic regulators and altered energy metabolisms (Figures 2D and 5D; Supplemental Figure S9B). Carbon and energy provision promotes nitrogen assimilation via transcriptional regulations when carbon skeleton is abundant and internal levels of organic nitrogen are insufficient (Matt et al., 2002; Foyer and Noctor, 2006). Sugar accumulation in the agb1-2 and wrky mutants can be considered as the prevention in root cells before being exposed to stress. In addition, the root phenotype of mutants may be mediated by phytohormones signaling (Smith and De Smet, 2012). Long-term exposure to mild drought stress leads to continuous root elongation through the

accumulation of ABA and BR (Gupta et al., 2020). Likewise, the ABA content and our transcriptomes from the agb1-2 and wrky40 alleles suggested genetic disruption of the ABA pathway (Figures 2C and 5C; Supplemental Figure S11), which possibly explains root growth regulations in the two alleles (Figure 6).

Taken together, this work revealed that plants use the crosstalk between AGB1 and WRKY TFs in common and specific stress responses. Root response to environmental changes involves metabolic adaptation and stress-responsive signaling that shapes root growth and architecture. Our study proposed the association between metabolic processes, stress-responsive signaling, and root morphology upon HN stress. Similar crosstalk may be present in plants to discriminate a variety of stress types through a combinatorial induction of WRKYs.

Materials and methods

Arabidopsis genetic materials

Arabidopsis (A. thaliana) T-DNA insertion lines were as previously described; agb1-2 (Ullah et al., 2003), gpa1-3 (Jones et al., 2003), agg3-3 (Chakravorty et al., 2011), agg1c-1/agg2-1 (Trusov et al., 2008), agg3-3/agg1c-1/agg2-1 (Thung et al., 2012), xlg1,2,3 (Ding et al., 2008), gpa1-3/xlg1,2,3 (Urano et al., 2016a), and wrky40 (Xu et al., 2006). Loss-of-function mutant for WRKY75 is SALK 101367, provided by Arabidopsis Biological Resource Center, USA. The AGB1/agb1-2 was kindly provided by Chakravorty et al. (2012). Overexpression of WRKY75 was done by cloning the coding sequence of AtWRKY75 from cDNA of Col-0 into pGWB552 using Gateway LR Clonase (Thermo Fisher Scientific, USA). Primers used for gene cloning are listed in Supplemental Table S5. The genetic transformation was done in agb1-2 according to floral dip protocol (Zhang et al., 2006) with Agrobacterium tumefaciens strain GV3101.

Sample collection for RNA sequencing, metabolic profiling, and quantification of ABA content

Sterilized Arabidopsis seeds were treated with 5-μM GA$_3$ for 3 d under darkness at 4°C. The seeds were washed 5 times with sterilized water and germinated on plant medium plates consisting of $1/2$ × Murashige-Skoog (MS), 1% w/v sucrose, 0.05% w/v MES, 0.8% w/v plant agar, pH 5.8 in a long-day chamber (16 h light/8 h darkness, 100 μmol m^{-2} s^{-1} and 22°C). Seven-day-old seedlings were transferred to plant liquid medium with or without 20-mM NH$_4$NO$_3$ and placed on an orbital shaker for 2 h in light condition. Root samples of around 50 seedlings were harvested in three biological replicates for RNA sequencing and metabolic profiling. One of the RNA-sequencing triplicates in wrky40 under control conditions was removed due to a large variation. Around 100 seedlings were collected in three biological replicates for quantification of ABA content.

Phenotyping assay

Four-day-old seedlings grown on plant medium plates were transferred to new plant medium plates supplemented with 0-, 5-, 10-, or 20-mM NH_4NO_3 (HN) or with DMSO or 2-μM ABA (ABA treated). Root tips were marked every 24 h for 6 d for the estimation of root elongation rate. The roots were imaged on Day 6. To evaluate root phenotypes in different sucrose concentrations under excess nitrogen, 4-d-old seedlings grown on plant medium plates without sucrose were used. Primary root length, number of lateral roots, leaf area, and chlorophyll index were measured by ImageJ with chlorophyll imager plugin (Liang et al., 2017).

Nitrate measurement

Nitrate content was evaluated as previously described (Zhao and Wang, 2017). In brief, 4-d-old seedlings were grown under various ammonium nitrate supplies for 6 d. Around 50 seedlings were harvested in three biological replicates. Frozen samples were ground with liquid nitrogen and boiled in water for 20 min. The sample solution was incubated with 5% salicylic acid in a concentrated sulfuric acid solution. Eight percent NaOH solution was added to the incubated sample before spectrophotometry measurement at A_{410}. Nitrate content was calculated based on the standard curve generated with potassium nitrate.

RNA-sequencing

Total RNA was isolated by RNeasy Plant Mini Kit, Qiagen, Germany. Library preparation including polyA enrichment, and sequencing of 150-bp paired-end reads on the Novoseq platform, was conducted by Novogene AIT Genomics, Singapore. Raw sequence reads were mapped to the *A. thaliana* (TAIR10) reference genome using STAR (v.2.5.3a) with default settings. Only uniquely mapped reads were processed for further analysis. DEGs were identified with the R package DESeq2. GO enrichment analysis was performed using AgriGO v.2 database (bioinfo.cau.edu.cn/agriGO). The redundant GO terms were removed by Revigo (revigo.irb.hr/). DEGs were identified using linear model: genotype + treatment + genotype*treatment with the threshold of $|log_2FC|$ >0.5 and FDR <0.1. Most of the DEGs (58%, ~1,700) showed greater effect under the interaction of genotype and treatment and therefore we mainly focused on those genes for downstream analysis. DEGs were further clustered by fuzzy c-means using mfuzz R package (Kumar and Futschik, 2007), resulting in 10 groups with unique expression patterns.

Metabolic profiling by GC-MS

Metabolite extraction, derivatization, and GC-MS condition were performed according to previously described (Lisec et al., 2006). Root extracts were separated using DB-35ms Ultra Inert column (30 m × 0.32 mm × 0.25 μm, Agilent, Santa Clara, CA, USA) with Agilent 7200 Q-TOF GCMS coupled to Agilent 7890B Gas Chromatograph by Chemical, Molecular and Materials Analysis Centre, National University of Singapore. Peak extraction and compound identification were performed by Mass Hunter Suite with default settings using the NIST 2014 mass spectral database.

Analysis of publicly available transcriptome dataset

Root expressed genes (~7,900) were taken as previously reported (Birnbaum et al., 2003). Ten microarrays (ATH1) experiments from six different abiotic stress using roots as material were retrieved from Genevestigator (https://genevestigator.com/). In each experiment, only the WT (Col-0) data comparing treatment to control condition were considered. It resulted in 23 datasets with 2–6 biological replicates for each dataset. Genes with adjusted $P < 0.05$ (treatment/control) were considered as DEGs and were selected for further analysis. Detailed sampling conditions for each experiment and DEGs identified from each stress were listed in Supplemental Table S1. GO term enrichment analysis was performed with AgriGO v.2 database (bioinfo.cau.edu.cn/agriGO) using standard settings. The redundant GO terms were removed by Revigo (revigo.irb.hr/). Significantly enriched GO terms (FDR < 0.05) were visualized as a heatmap in R software.

Motif enrichment analysis

AME from MEME suite (McLeay and Bailey, 2010) was used to identify enriched TF binding motifs in the 2-kb region upstream from the transcription start site of genes assigned to each DEG group containing genotype-specific genes. The parameters were set as follows: --verbose 1 --scoring avg --method fisher --hit-lo-fraction 0.25 --evalue-report-threshold 10.0 --control --shuffle-- --kmer 2. Arabidopsis DAP-Seq database (O'Malley et al., 2016) was used as a reference.

RNA extraction, cDNA synthesis, and RT-qPCR

Total RNA was extracted from Arabidopsis roots using RNeasy Plant Mini Kit (Qiagen, Hilden, Germany). First-strand cDNA was synthesized using iScript cDNA Synthesis Kit (Biorad, Hercules, CA, USA). Quantitative gene expression analysis (RT-qPCR) was performed as previously described (Wu et al., 2013). Data were analyzed according to the manufacturer's instructions using the CFX ManagerTM v3.1 (Bio-Rad). Gene expression level was normalized using the expression of *Arabidopsis ACTIN 2* (AtACT2). The primers used are listed in Supplemental Table S5.

Quantification of ABA by LC-MS/MS

Quantification of ABA content was carried out based on previously described (Vidal et al., 2018) with modification. Around 200 mg of seedling were ground in liquid nitrogen and suspended in 80% methanol–1% acetic acid. Samples were shaken constantly at 4°C for 1 h followed by overnight incubation at −20°C. The supernatants were passed through Oasis Prime HLB (Waters) and dried with a vacuum evaporator. The dried eluate was dissolved in 50% methanol–1% acetic acid. Extracts were separated by UPLC chromatography (Acquity UPLC BEH C18, 1.7 μm, 2.1 × 100 mm, Waters) with 5%–50% acetonitrile gradient containing 0.05% acetic acid, at 400 μL min^{-1} over 14 min. ABA content was

analyzed by Q-Exactive mass spectrometry (Orbitrap detector, ThermoFisher Scientific) by MS^2 mode. The concentration of ABA was determined using standard calibration curves.

Accession numbers

Sequence data of the gene from this article can be found in the GenBank/EMBL data libraries under gene ID as shown in Supplemental Table S5. RNA-seq data are deposited in GEO under accession number GSE184528.

Supplemental data

The following materials are available in the online version of this article.

Supplemental Figure S1. GO terms enriched in DEGs specific to individual abiotic stresses.

Supplemental Figure S2. Common abiotic and HN-specific responses under HN treatment.

Supplemental Figure S3. GO enrichment analysis of DEGs belonging to common stress response.

Supplemental Figure S4. Root growth of *AGB1/agb1-2*, Col-0, and *agb1-2* in response to different nitrogen supplies.

Supplemental Figure S5. Lateral root density of Col-0 and *agb1-2* in different nitrogen supplies.

Supplemental Figure S6. Root elongation rate of G protein mutants under different nitrogen conditions.

Supplemental Figure S7. Leaf area, chlorophyll index, and nitrate content of seedlings.

Supplemental Figure S8. TF families and pCRE enrichment in response to HN and WRKYs expression in response to abiotic stresses.

Supplemental Figure S9. Metabolic response of Col-0, *agb1-2*, *wrky40*, and *wrky75* to HN.

Supplemental Figure S10. Relative expression of metabolic and ABA-related genes in roots of *agb1-2* and *wrky* mutants.

Supplemental Figure S11. ABA content of Col-0, *agb1-2*, *wrky40*, *wrky75*, and OEWRKY75|*agb1-2* in response to HN.

Supplemental Table S1. Detailed sampling conditions for abiotic stresses experiment and list of DEGs in response to abiotic stresses: cold, drought, hypoxia, heat, osmotic, and salt.

Supplemental Table S2. List of DEGs in each of the gene groups clustered by mfuzz.

Supplemental Table S3. Number and percentage of DEGs in each gene group showing differential expression across genotypes/conditions using cut off at $|\log_2 FC| < 0.5$ and FDR < 0.1.

Supplemental Table S4. The abundance of metabolites obtained from GC-MS analysis in the root of Col-0, *agb1-2*, *wrky40*, and *wrky75* at 0 and 2 h of NH_4NO_3 supplement.

Supplemental Table S5. Primer sequence for quantitative gene expression analysis shown in Figure 6 and *WRKY75* cloning.

References

Akram R, Fahad S, Masood N, Rasool A, Ijaz M, Ihsan MZ, Maqbool MM, Ahmad S, Hussain S, Ahmed M, et al. (2019) Plant growth and morphological changes in rice under abiotic stress. *In* M Hasanuzzaman, M Fujita, K Nahar, JK Biswas, eds, Advances in Rice Research for Abiotic Stress Tolerance. Elsevier, Amsterdam, The Netherlands, pp 69–85

Birkenbihl RP, Kracher B, Somssich IE (2017) Induced genome-wide binding of three Arabidopsis WRKY transcription factors during early MAMP-triggered immunity. Plant Cell **29**: 20

Birnbaum K, Shasha DE, Wang JY, Jung JW, Lambert GM, Galbraith DW, Benfey PN (2003) A gene expression map of the Arabidopsis root. Science **302**: 1956–1960

Chakravorty D, Trusov Y, Botella JR (2012) Site-directed mutagenesis of the Arabidopsis heterotrimeric G protein β subunit suggests divergent mechanisms of effector activation between plant and animal G proteins. Planta **235**: 615–627

Chakravorty D, Trusov Y, Zhang W, Acharya BR, Sheahan MB, McCurdy DW, Assmann SM, Botella JR (2011) An atypical heterotrimeric G-protein γ-subunit is involved in guard cell K + -channel regulation and morphological development in *Arabidopsis thaliana*. Plant J **67**: 840–851

Cramer GR, Urano K, Delrot S, Pezzotti M, Shinozaki K (2011) Effects of abiotic stress on plants: A systems biology perspective. BMC Plant Biol **11**: 1–14

Cui G, Zhang Y, Zhang W, Lang D, Zhang X, Li Z, Zhang X (2019) Response of carbon and nitrogen metabolism and secondary metabolites to drought stress and salt stress in plants. J Plant Biol **62**: 387–399

Desnos T (2008) Root branching responses to phosphate and nitrate. Curr Opin Plant Biol **11**: 82–87

Devaiah BN, Karthikeyan AS, Raghothama KG (2007) WRKY75 transcription factor is a modulator of phosphate acquisition and root development in Arabidopsis. Plant Physiol **143**: 1789–1801

Ding L, Pandey S, Assmann SM (2008) Arabidopsis extra-large G proteins (XLGs) regulate root morphogenesis. Plant J **53**: 248–263

Foyer CH, Noctor G (2006) Photosynthetic Nitrogen Assimilation and Associated Carbon and Respiratory Metabolism. Springer Science & Business Media, New York, USA.

Gou T, Yang L, Hu W, Chen X, Zhu Y, Guo J, Gong H (2020) Silicon improves the growth of cucumber under excess nitrate stress by enhancing nitrogen assimilation and chlorophyll synthesis. Plant Physiol Biochem **152**: 53–61

Gounaris Y (2001) A qualitative model for the mechanism of sugar accumulation in cold-stressed plant tissues. Theory Biosci **120**: 149–165

Gruber BD, Giehl RFH, Friedel S, von Wirén N (2013) Plasticity of the Arabidopsis root system under nutrient deficiencies. Plant Physiol 163: 161–179

Gupta A, Sinha R, Fernandes JL, Abdelrahman M, Burritt DJ, Tran L-SP (2020) Phytohormones regulate convergent and divergent responses between individual and combined drought and pathogen infection. Crit Rev Biotechnol 40: 320–340

Heinemann B, Hildebrandt TM (2021) The role of amino acid metabolism in signaling and metabolic adaptation to stress-induced energy deficiency in plants. J Exp Bot 72: 4634–4645

Hirano T, Satoh Y, Ohki A, Takada R, Arai T, Michiyama H (2008) Inhibition of ammonium assimilation restores elongation of seminal rice roots repressed by high levels of exogenous ammonium. Physiol Plant 134: 183–190

Hu Y, Dong Q, Yu D (2012) Arabidopsis WRKY46 coordinates with WRKY70 and WRKY53 in basal resistance against pathogen *Pseudomonas syringae*. Plant Sci 185–186: 288–297

Hu Y, Schmidhalter U (2005) Drought and salinity: a comparison of their effects on mineral nutrition of plants. J Plant Nutr Soil Sci 168: 541–549

Huang L, Hong Y, Zhang H, Li D, Song F (2016) Rice NAC transcription factor ONAC095 plays opposite roles in drought and cold stress tolerance. BMC Plant Biol 16: 203

Jiang J, Ma S, Ye N, Jiang M, Cao J, Zhang J (2017) WRKY transcription factors in plant responses to stresses. JIntegr Plant Biol 59: 86–101

Jones AM, Ecker JR, Chen J-G (2003) A reevaluation of the role of the heterotrimeric G protein in coupling light responses in Arabidopsis. Plant Physiol 131: 1623–1627

Kalde M, Barth M, Somssich IE, Lippok B (2007) Members of the Arabidopsis WRKY Group III transcription factors are part of different plant defense signaling pathways. Mol Plant Microbe Interact 16: 295–305

Koevoets IT, Venema JH, Elzenga JTM, Testerink C (2016) Roots withstanding their environment: Exploiting root system architecture responses to abiotic stress to improve crop tolerance. Front Plant Sci 7: 1335

Kong L, Xie Y, Hu L, Si J, Wang Z (2017) Excessive nitrogen application dampens antioxidant capacity and grain filling in wheat as revealed by metabolic and physiological analyses. Sci Rep 7: 43363

Konishi M, Yanagisawa S (2013) An NLP-binding site in the 3′ flanking region of the nitrate reductase gene confers nitrate-inducible expression in *Arabidopsis thaliana* (L.) Heynh. Soil Sci Plant Nutr 59: 612–620

Kumar L, Futschik ME (2007) Mfuzz: A software package for soft clustering of microarray data. Bioinformation 2: 5

Lan G, Jiao C, Wang G, Sun Y, Sun Y (2020) Effects of dopamine on growth, carbon metabolism, and nitrogen metabolism in cucumber under nitrate stress. Sci Hortic (Amsterdam) 260: 108790

Liang X, Ding P, Lian K, Wang J, Ma M, Li L, Li L, Li M, Zhang X, Chen S, et al. (2016) Arabidopsis heterotrimeric G proteins regulate immunity by directly coupling to the FLS2 receptor. eLife 5: e13568

Liang Y, Urano D, Liao K-L, Hedrick TL, Gao Y, Jones AM (2017) A nondestructive method to estimate the chlorophyll content of Arabidopsis seedlings. Plant Methods 13: 26

Liang Y, Zhao X, Jones AM, Gao Y (2018) G proteins sculp root architecture in response to nitrogen in rice and Arabidopsis. Plant Sci 274: 129–136

Lisec J, Schauer N, Kopka J, Willmitzer L, Fernie AR (2006) Gas chromatography mass spectrometry–based metabolite profiling in plants. Nat Protoc 1: 387–396

López-Ruiz BA, Zluhan-Martínez E, Sánchez M de la P, Álvarez-Buylla ER, Garay-Arroyo A (2020) Interplay between hormones and several abiotic stress conditions on *Arabidopsis thaliana* primary root development. Cells 9: 2576

Ma S, Bohnert HJ (2007) Integration of *Arabidopsis thaliana* stress-related transcript profiles, promoter structures, and cell-specific expression. Genome Biol 8: R49

Matt P, Krapp A, Haake V, Mock H-P, Stitt M (2002) Decreased Rubisco activity leads to dramatic changes of nitrate metabolism, amino acid metabolism and the levels of phenylpropanoids and nicotine in tobacco antisense RBCS transformants. Plant J 30: 663–677

McLeay RC, Bailey TL (2010) Motif enrichment analysis: A unified framework and an evaluation on ChIP data. BMC Bioinforma 11: 1–11

Mudgil Y, Karve A, Teixeira PJPL, Jiang K, Tunc-Ozdemir M, Jones AM (2016) Photosynthate regulation of the root system architecture mediated by the heterotrimeric g protein complex in Arabidopsis. Front Plant Sci 7: 1255

O'Malley RC, Huang SSC, Song L, Lewsey MG, Bartlett A, Nery JR, Galli M, Gallavotti A, Ecker JR (2016) Cistrome and epicistrome features shape the regulatory DNA landscape. Cell 165: 1280–1292

Offermanns S (2003) G-proteins as transducers in transmembrane signalling. Prog Biophys Mol Biol 83: 101–130

Pandey S, Chen J-G, Jones AM, Assmann SM (2006) G-protein complex mutants are hypersensitive to abscisic acid regulation of germination and postgermination development. Plant Physiol 141: 243–256

Pandey S, Wang R-S, Wilson L, Li S, Zhao Z, Gookin TE, Assmann SM, Albert R (2010) Boolean modeling of transcriptome data reveals novel modes of heterotrimeric G-protein action. Mol Syst Biol 6: 372

Poza-Carrión C, Paz-Ares J (2019) When nitrate and phosphate sensors meet. Nat Plants 5: 339–340

Savchenko T, Tikhonov K (2021) Oxidative stress-induced alteration of plant central metabolism. Life 11: 304

Schläpfer P, Zhang P, Wang C, Kim T, Banf M, Chae L, Dreher K, Chavali AK, Nilo-Poyanco R, Bernard T, et al. (2017) Genome-wide prediction of metabolic enzymes, pathways, and gene clusters in plants. Plant Physiol 173: 2041–2059

Shang Y, Yan L, Liu Z-Q, Cao Z, Mei C, Xin Q, Wu F-Q, Wang X-F, Du S-Y, Jiang T, et al. (2010) The Mg-chelatase H subunit of Arabidopsis antagonizes a group of WRKY transcription repressors to relieve ABA-responsive genes of inhibition. Plant Cell 22: 1909–1935

Shinozaki K, Yamaguchi-Shinozaki K (2000) Molecular responses to dehydration and low temperature: differences and cross-talk between two stress signaling pathways. Curr Opin Plant Biol 3: 217–223

Smith S, De Smet I (2012) Root system architecture: Insights from Arabidopsis and cereal crops. Philos Trans R Soc B Biol Sci 367: 1441–1452

Tang D, Mao L, Zhi YE, Zhang J-Z, Zhou P, Chai X-T (2014) Investigation and canonical correspondence analysis of salinity contents in secondary salinization greenhouse soils in Shanghai suburb. Huan jing ke xue Huanjing kexue 35: 4705–4711

Tao Z, Kou Y, Liu H, Li X, Xiao J, Wang S (2011) OsWRKY45 alleles play different roles in abscisic acid signalling and salt stress tolerance but similar roles in drought and cold tolerance in rice. J Exp Bot 62: 4863–4874

Thung L, Trusov Y, Chakravorty D, Botella JR (2012) Gγ1 + Gγ2 + Gγ3 = Gβ: The search for heterotrimeric G-protein γ subunits in Arabidopsis is over. J Plant Physiol 169: 542–545

Trusov Y, Zhang W, Assmann SM, Botella JR (2008) Gγ1 + Gγ2 ≠ Gβ: Heterotrimeric G protein Gγ-deficient mutants do not recapitulate all phenotypes of Gβ-deficient mutants. Plant Physiol 147: 636–649

Ullah H, Chen J-G, Temple B, Boyes DC, Alonso JM, Davis KR, Ecker JR, Jones AM (2003) The β-subunit of the Arabidopsis G protein negatively regulates auxin-induced cell division and affects multiple developmental processes. Plant Cell 15: 393–409

Urano D, Chen J-G, Botella JR, Jones AM (2013) Heterotrimeric G protein signalling in the plant kingdom. Open Biol 3: 120186

Urano D, Maruta N, Trusov Y, Stoian R, Wu Q, Liang Y, Jaiswal DK, Thung L, Jackson D, Botella JR, et al. (2016a) Saltational

evolution of the heterotrimeric G protein signaling mechanisms in the plant kingdom. Sci Signal **9**: ra93

Urano D, Miura K, Wu Q, Iwasaki Y, Jackson D, Jones AM (2016b) Plant morphology of heterotrimeric G protein mutants. Plant Cell Physiol **57**: 437–445

Verma V, Ravindran P, Kumar PP (2016) Plant hormone-mediated regulation of stress responses. BMC Plant Biol **16**: 1–10

Vidal A, Cantabella D, Bernal-Vicente A, Díaz-Vivancos P, Hernández JA (2018) Nitrate- and nitric oxide-induced plant growth in pea seedlings is linked to antioxidative metabolism and the ABA/GA balance. J Plant Physiol **230**: 13–20

Wei GP, Yang LF, Zhu YL, Chen G (2009) Changes in oxidative damage, antioxidant enzyme activities and polyamine contents in leaves of grafted and non-grafted eggplant seedlings under stress by excess of calcium nitrate. Sci Hortic (Amsterdam) **120**: 443–451

Wu T, Juan Y, Hsu Y, Wu S, Liao H, Fung RWM, Charng Y (2013) Interplay between heat shock proteins HSP101 and HSA32 prolongs heat acclimation memory posttranscriptionally in Arabidopsis. Plant Physiol **161**: 2075–2084

Wu T-Y, Goh H, Azodi CB, Krishnamoorthi S, Liu M-J, Urano D (2021) Evolutionarily conserved hierarchical gene regulatory networks for plant salt stress response. Nat Plants **7**: 787–799

Wu T-Y, Krishnamoorthi S, Goh H, Leong R, Sanson AC, Urano D (2020) Crosstalk between heterotrimeric G protein-coupled signaling pathways and WRKY transcription factors modulating plant responses to suboptimal micronutrient conditions. J Exp Bot **71**: 3227–3239

Wu T-Y, Urano D (2018) Genetic and systematic approaches toward G protein-coupled abiotic stress signaling in plants. Front Plant Sci **9**: 1378

Xin W, Zhang L, Zhang W, Gao J, Yi J, Zhen X, Li Z, Zhao Y, Peng C, Zhao C (2019) An integrated analysis of the rice transcriptome and metabolome reveals differential regulation of carbon and nitrogen metabolism in response to nitrogen availability. Int J Mol Sci **20**: 2349

Xu X, Chen C, Fan B, Chen Z (2006) Physical and functional interactions between pathogen-induced Arabidopsis WRKY18, WRKY40, and WRKY60 transcription factors. Plant Cell **18**: 1310–1326

Xuan YH, Priatama RA, Huang J, Je B Il, Liu JM, Park SJ, Piao HL, Son DY, Lee JJ, Park SH, et al. (2013) Indeterminate domain 10 regulates ammonium-mediated gene expression in rice roots. New Phytol **197**: 791–804

Yastreb TO, Kolupaev YE, Lugovaya AA, Dmitriev AP (2016) Content of osmolytes and flavonoids under salt stress in *Arabidopsis thaliana* plants defective in jasmonate signaling. Appl Biochem Microbiol **52**: 210–215

Yu Y, Assmann SM (2015) The heterotrimeric G-protein β subunit, AGB1, plays multiple roles in the Arabidopsis salinity response. Plant Cell Environ **38**: 2143–2156

Zhang X, Henriques R, Lin S-S, Niu Q-W, Chua N-H (2006) Agrobacterium-mediated transformation of *Arabidopsis thaliana* using the floral dip method. Nat Protoc **1**(2): 641–646

Zhang X, Wang B, Zhao Y, Zhang J, Li Z (2019) Auxin and GA signaling play important roles in the maize response to phosphate deficiency. Plant Sci **283**: 177–188

Zhao L, Wang Y (2017) Nitrate assay for plant tissues. Bio-protocol **7**. doi: 10.21769/BIOPROTOC.2029

Zou N, Li B, Dong G, Kronzucker HJ, Shi W (2012) Ammonium-induced loss of root gravitropism is related to auxin distribution and TRH1 function, and is uncoupled from the inhibition of root elongation in Arabidopsis. J Exp Bot **63**: 3777–3788